

# INTEGRATED APPROACH FOR ESTIMATION AND RESTORATION OF PHOTON-LIMITED IMAGES BASED ON STEERABLE PYRAMIDS

Filip Rooms<sup>1</sup>, Wilfried Philips<sup>1</sup> and Patrick Van Oostveldt<sup>2</sup>

Ghent University

<sup>1</sup> Department of Telecommunications and Information Processing

Sint-Pietersnieuwstraat 41, B-9000 Ghent, Belgium

Filip.Rooms@telin.rug.ac.be      <http://telin.rug.ac.be/~frooms/>

Tel. +32 9 264 34 15      Fax. +32 9 264 42 95

<sup>2</sup> Department Molecular Biotechnology, Coupure Links 653, B-9000 Gent, Belgium

patrick.vanoostveldt@rug.ac.be      <http://biochema.rug.ac.be/>

## Abstract

*In disciplines like fluorescence microscopy and astronomical imaging, the imaging process is based on detection of photons. Fluctuations in photon counting processes are described by Poisson statistics. In this paper, a new combined method based on steerable pyramids is proposed for the estimation of the degradation parameters (like noise and blur) and the restoration of photon-limited images. It consists of the following steps: in the steerable pyramid domain, a noise suppression step is performed, followed by a blur estimation. As a last step, the Richardson-Lucy deconvolution algorithm is applied. These steps are iterated. The only free parameter in the algorithm is the number of iterations, but an empirical stopping rule is suggested in terms of the blur estimation. Otherwise, this method is fully automatic and provides very nice restoration results.*

**Keywords:** *Richardson-Lucy deconvolution, wavelet shrinkage, Poisson noise, Anscombe transform, automatic.*

## 1 INTRODUCTION

Images are produced to record and visualize information. The available information is usually degraded by the observation process, which consists of blurring due to a band limited imaging process (like an optical system), as well as a noise process, which can be due to the recording process by some detector (like a PMT or a CCD). Image degradation is usually modeled as:

$$g(x, y) = N((h * f)(x, y))$$

with  $g(x, y)$  the blurred image,  $f(x, y)$  the unknown ideal image and  $h(x, y)$  the Point Spread Function (PSF). The symbol  $*$  represents the convolution operator, and models the image blur. The function  $N(\cdot)$  represents the noise processes, caused by the quantum nature of the photon detection process.

The goal of image restoration is to recover  $f(x, y)$  as well as possible from a degraded observed image  $g(x, y)$ . When the degradation parameters (in particular the PSF) are known, one has a classical image restoration problem [1]. However, in some cases the degradation parameters are unknown, and one has two choices: estimating the signal of interest and the degradation parameters simultaneously (blind restoration [2]), or estimating the degradation parameters before starting the restoration process [3]. This paper follows the latter approach.

In this paper, we present a combined method for degradation estimation and image restoration and that is based on steerable pyramids [4, 5]. To our knowledge, it is the first joint approach for degradation estimation and regularization of deconvolution with steerable pyramids. Only the deconvolution itself isn't calculated with steerable pyramids. In the process some nontrivial problems had to be solved to integrate the different techniques into one framework. Our combined method outperforms clearly normal Richardson-Lucy (RL deconvolution, which is commonly used for restoration of photon-limited images.

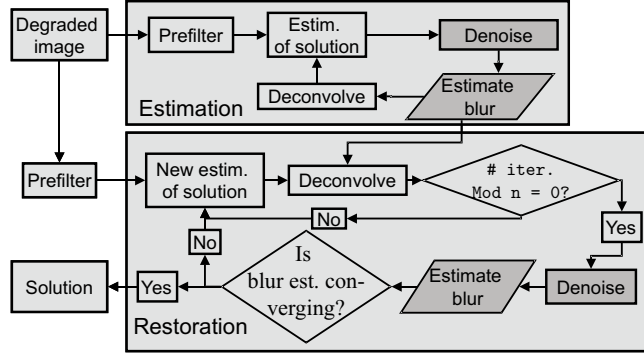


Figure 1. The flowchart of the algorithm. Steps in dark gray are executed in the steerable pyramid domain.

## 2 OUTLINE OF THE ALGORITHM

The algorithm starts with a steerable pyramid decomposition of the image, followed by noise reduction in the transformed domain. From the noise-reduced subbands, the blur is estimated. After this step, the filtered subbands of the steerable pyramid are recombined. Finally, a Richardson-Lucy deconvolution is applied on the prefiltered image. These different steps are repeated for a number of times. The estimation of the blur is stable after two iterations, and is used unaltered from then on in each deconvolution step. After this training process, the iterations are restarted with the original degraded image, and the blur estimation is used to control the number of iterations (see fig. 4 (d)): when the blur estimation converges, the iterations are stopped. Also, regularization can be imposed every  $n$  iterations ( $\# \text{ iter. mod } n = 0$ ), instead of imposing it every iteration. We show results how often regularization is required in the process.

We will first focus on the steerable pyramid transform, followed by a more detailed explanation of the different steps of the algorithm.

### 2.1 Introduction to steerable pyramids.

In computer vision, one often wants to analyse oriented image structures, like edges under a certain angle. One could filter the image with a range of oriented kernels which cover the whole continuum of angles present in the image. However, this would demand a high computational cost.

In literature, it is shown that one can restrict the computations to filter the image with a fixed set of basic kernels, and interpolate the image filtered with a kernel under an arbitrary direction from the results of the image filtered with the basic kernels [4, 5]. Such a set of kernels is called a steerable filter set. The most illustrative example [5] is a kernel computed as the first partial derivatives in  $x$  and  $y$  of the Gaussian function  $G(x, y) = e^{-(x^2+y^2)} = e^{-r^2}$ .

The partial derivative in  $x$  is given by  $G'_x(x, y) = -2x e^{-r^2}$  and in  $y$  by  $G'_y(x, y) = -2y e^{-r^2}$ . The kernels  $G'_x$  and  $G'_y$  can be interpreted as filters for horizontal and vertical image features respectively. Let  $I(x, y)$  be the original image and let the symbol  $*$  again be the convolution operator. Then  $R_x(x, y) = (I * G'_x)(x, y)$  is the image filtered for vertical features and  $R_y(x, y) = (I * G'_y)(x, y)$  for horizontal features. These two kernels form a steerable basis set: to compute a kernel  $G'_\theta(x, y)$  to analyse features under an arbitrary angle  $\theta$ , one can take a linear combination of the two basic kernels:

$$G'_\theta(x, y) = \cos(\theta) G'_x(x, y) + \sin(\theta) G'_y(x, y) \quad (1)$$

To calculate  $R_\theta(x, y)$  for a large number of different values of  $\theta$  would be computationally expensive. However, because convolution is a linear operation, it is sufficient to calculate  $R_\theta(x, y)$  as a linear combination of the original image filtered with the two basic kernels:

$$R_\theta(x, y) = \cos(\theta) R_x(x, y) + \sin(\theta) R_y(x, y)$$

which is computationally far less expensive. In [4], the general conditions were given for a set of kernels to be steerable. In [5], the steerable pyramid is described. This decomposition based on steerable filters is similar to a wavelet decomposition, but has a much better orientation resolution.

To design the steerable pyramid, we based on the principles in [5] and the practical design on [6]. For this design, the Fourier domain is divided into a set of transfer functions. We start with an initial highpass fraction  $H_0$  and a lowpass fraction  $L_0$ . This fraction  $L_0$  is then divided in a bandpass fraction  $M1$  and a second lowpass

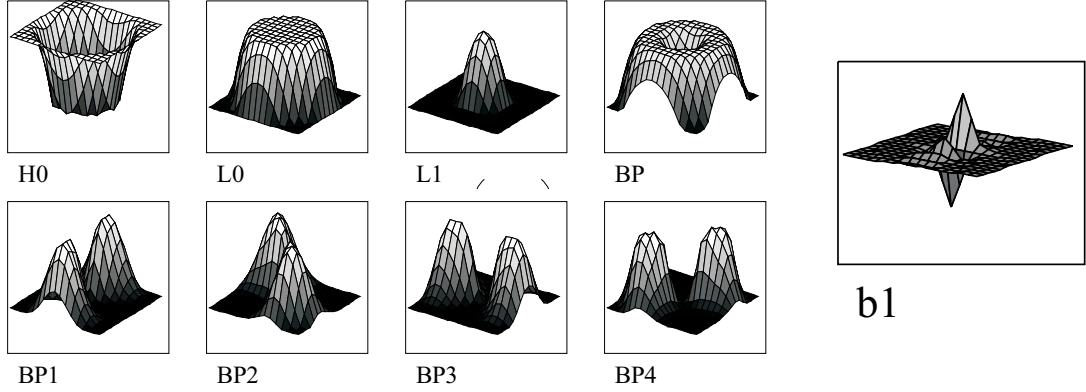


Figure 2. Transfer functions of steerable pyramid (left) and example of a basic kernel  $b_1$  (right) (based on Matcadfiles of Castleman [6])

$L_1$  (see top row of fig. 2). Each bandpass is subdivided in oriented bandpass fractions. In the example with formula 1, only two bandpass fractions were used, which limits the orientation resolution. We use 4 oriented subbands  $BP_1$  to  $BP_4$  (bottom row of figure 2). For the next level,  $L_1$  is again subdivided in a subband and a lowpass fraction. Once the transfer functions are defined, the filter kernels are computed using the inverse fourier transform and provide nearly perfect FIR filters (fig. 2,  $b_1$ ).

## 2.2 Noise reduction

In photon-limited imaging, the major source of errors is Poisson noise due to the discrete nature of photon detection. Unlike Gaussian noise, Poisson noise is signal dependent, which makes separating signal from noise a very difficult task [7]. However, by applying the Anscombe transform [8], the Poisson data are transformed to data with a Gaussian distribution with  $\sigma = 1$ . The Anscombe transform is given by:

$$t(I(x, y)) = 2\sqrt{I(x, y) + \frac{3}{8}}$$

with  $I(x, y)$  data determined by a Poisson process. This transformation allows to use well studied methods for Gaussian noise on data with the much trickier Poisson noise. Then we applied the shrinkage method developed for Gaussian data by Şendur [9], where a bivariate wavelet shrinkage function is proposed:

$$\hat{w}_1(k) = \frac{\left(\sqrt{y_1^2(k) + y_2^2(k)} - \frac{\sqrt{3}\sigma_n^2}{\sigma(k)}\right)_+}{\sqrt{y_1^2(k) + y_2^2(k)}}$$

A denoised coefficient  $\hat{w}_1(k)$  is calculated by using the corresponding noisy coefficient  $y_1(k)$  and its parent  $y_2(k)$ , the coefficient at the same spatial position as  $y_1(k)$ , but in the next coarser resolution scale.  $\sigma_n^2$  denotes the noise variance, and  $\hat{\sigma}$  denotes the marginal variance for the  $k^{th}$  coefficient (see [9] for details). The operator  $(\cdot)_+$  returns the result of the expression if it's positive, or zero if the result is negative. This algorithm provides a good noise reduction performance, and we adapted it for implementation with steerable pyramids. After denoising, the inverse Anscombe transform was applied.

## 2.3 Blur estimation

Our own method for blur estimation also operates in the steerable pyramid domain, and is based on estimating the sharpness of the sharpest edges in the image. To analyse edges in the image, we calculate the evolution of the wavelet modulus maxima through scales. Mallat has shown in [10] that this evolution through scales depends on three factors:

- the regularity of the original underlying signal (was it a step edge or a smooth transition?)
- the properties of the wavelet basis functions used in the transform
- the blur of the signal at position  $k$

This means that the blur can be estimated from the evolution of the wavelet coefficients through scales when the other factors are known.

To achieve this, we located the modulus maxima of the coefficients of the steerable pyramid in the highest resolution scale and followed the evolution of their magnitude through the different resolution scales. By fitting a curve to each of these series of modulus maxima, we obtained a local measure for the blur in the image. Assuming that the PSF is Gaussian, spatially independent and rotationally invariant, we averaged out the blur measures for the different edge pixels to obtain a robust estimate for the variance of the PSF. This method also works for parametric PSF's other than the Gaussian. According to our knowledge, it's the first time that the evolution of wavelet coefficients through scales is used to estimate image blur.

## 2.4 Deconvolution step

As a deconvolution step, the Richardson-Lucy algorithm [11] was used. The origin of this algorithm was laid by Dempster. It was first applied in image reconstruction by Shepp and Vardi. The algorithm is identical to the algorithms independently obtained by Richardson and Lucy. More information and references can be found in [11].

The algorithm can be derived in a Bayesian context by considering pure Poisson noise and taking a constant as prior information. The Richardson-Lucy algorithm has an iterative scheme of the form:

$$\hat{f}_{k+1} = \hat{f}_k \left[ h^* * \frac{g}{h * \hat{f}_k} \right]$$

where  $\hat{f}_{k+1}$  indicates a new estimate of the image,  $g$  represents the observed, degraded data and  $h$  is the Point Spread Function. This algorithm has following main properties [8]:

- Each estimation  $\hat{f}_k$  is guaranteed to contain only nonnegative pixels
- The sum of the intensities over the whole image is preserved during each iteration
- The log-likelihood of the solution is non-decreasing during the iterations, and converges to a maximum.

## 2.5 Stopping rule and how often to regularize.

In this section, we briefly discuss when to stop the iterations and how often regularization is required. We noticed that the estimation of the blur is decreasing in function of the number of iterations (as expected), as the likelihood of the solution is increasing (illustrated in fig. 4(d) with an experiment with the confocal image). As an empirical rule, we stop the iterations when the ratio of the blur estimated during previous iteration  $\sigma_{blur,i-1}$  and iteration current  $i$  is converging to 1, i.e., when  $|\frac{\sigma_{blur,i-1}}{\sigma_{blur,i}} - 1| < \epsilon$ , with  $\epsilon$  an empirical threshold chosen to be 0.01.

The calculation of the steerable pyramid is computational intensive, so we would like to minimize the number of transformations to and from the steerable pyramid domain. It is clear that the more often the solution is regularized, the smoother the solution is. In fact, regularizing every iteration may oversmoothen the result, therefore regularizing every two or three iterations was chosen.

## 2.6 Experimental results

We degraded a synthetic test image with a Gaussian PSF with a  $\sigma_{blur}$  of 3 pixels, followed by corrupting the image with Poisson noise. In fig. 3(a), the test image is shown, fig. 3(b) shows the degraded image. Fig. 3(c) gives the result of restoration using the classical Richardson-Lucy (RL) algorithm without any regularization. In Fig. 3(d) slight postblurring after each iteration is applied (as used in some confocal image restoration packages). For (c) and (d), the true PSF was used. Fig. 3(e) is the result of our own method, with regularization after every iteration, (f) after every three iterations and (g) after every eight iterations. Notice that the noise is better suppressed (less artefacts) and that the image is sharper after the same number of iterations with our method. Also, regularization every three iterations shows to be sufficient.

In fig. 4, we apply our method on a real confocal microscope image of a human cell in mitose, treated with a microtubuli stabilizing agent (the dividing nucleus is shown at the lower right). The arc-like structure is the cytoskeleton. Here, fig. 4(a) is the raw image, fig. 4(b-c) is the result with classical RL (resp. without and with postblurring) and fig. 4(d-f) are the results with our own method ((d) regularization every iteration, (e) every 2 it. and (f) every 3 it.). Notice also here that noise is better suppressed (less artefacts) with our method than with the classical algorithm. For this image, no PSF was available, so a synthetic PSF from the first blur

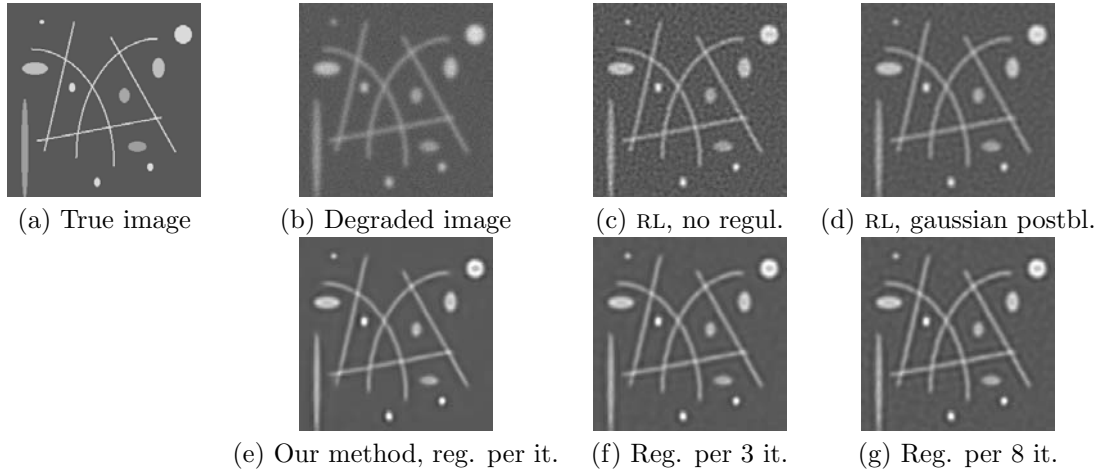


Figure 3. Restoration of degraded synthetic test image.

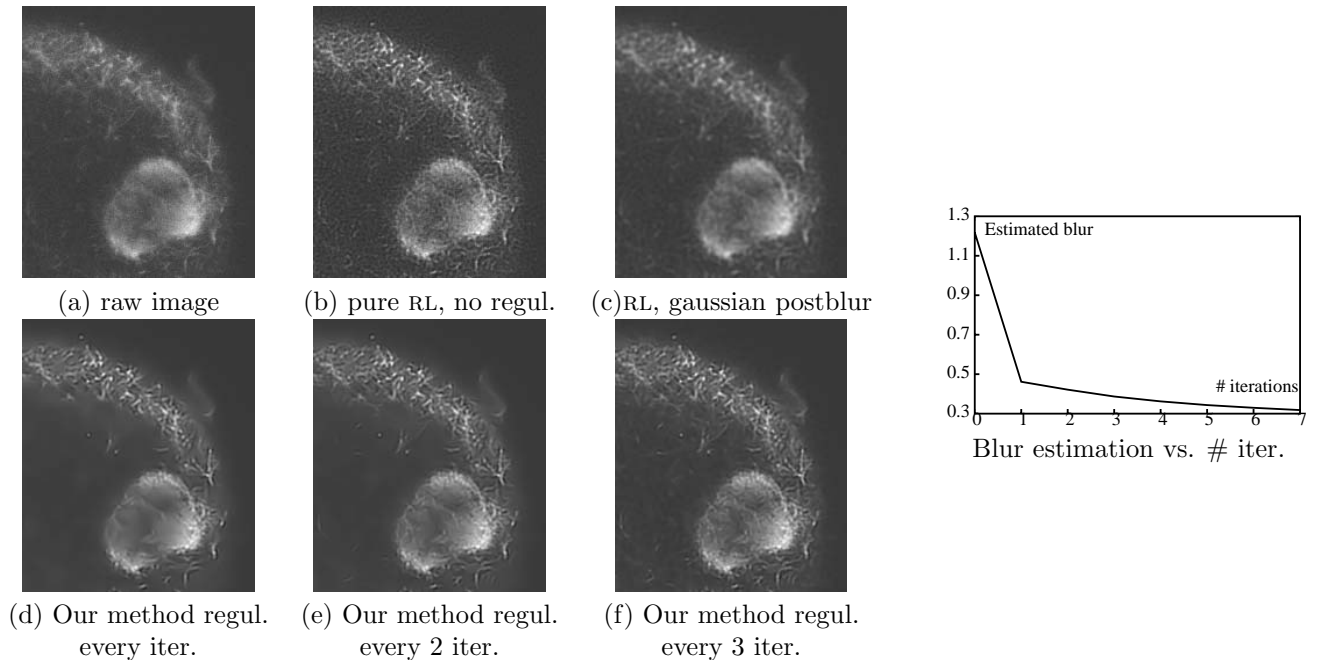


Figure 4. Restoration of a real confocal microscope image.

estimation was used. In fig. 4(d), we plot the blur estimation vs. the number of iterations. Regularization every iteration here oversmoothens the image, so applying it every two iterations is better. When only applied every three iterations, disturbing artefacts are visible.

### 3 CONCLUSIONS AND FUTURE WORK

In this paper, we present an integrated stable and automatic framework to restore degraded photon-limited images. The estimation of the degradation parameters as well as the regularization of the deconvolution are performed in the steerable pyramid domain. The blur estimation is used to formulate a stop criterion for the iterations, thus making the restoration fully automatic. Regularization is also not required every iteration.

Future work will also include the deconvolution step in the steerable pyramid domain, as well as the estimation of less symmetric PSF's.

### 4 ACKNOWLEDGEMENTS

This research was financed with specialisation scholarship of the Flemish Institute for Stimulation of Scientific-Technical research in the industry (IWT). Image 4 was recorded by prof. dr. P. Van Oostveldt of the

Lab. Biochemistry and Molecular Cytology at the Faculty of Agricultural and Applied Biological Sciences of Ghent University.

## REFERENCES

- [1] M. Bertero and P. Boccacci, *Introduction to inverse problems in imaging*, Institute of Physics Publishing, Bristol and Philadelphia, 1998.
- [2] D. Kundur and D. Hatzinakos, "Blind image deconvolution," *IEEE Signal Processing Magazine*, vol. 13, no. 3, pp. 43–64, May 1996.
- [3] A. K. (ed.) Katsaggelos, *Digital Image Restoration*, Springer-Verlag, Berlin, Heidelberg, New York, 1989.
- [4] W. T. Freeman and E. H. Adelson, "The design and use of steerable filters," *IEEE Trans. Pattern Analysis and Machine Intelligence*, vol. 13, no. 9, pp. 891–906, 1991.
- [5] E. P. Simoncelli, W. T. Freeman, E. H. Adelson, and D. J. Heeger, "Shiftable multi-scale transforms," *IEEE Trans. Informations Theory*, vol. 38, no. 2, 1992.
- [6] K. R. Castleman, M. A. Schulze, and Q. Wu, "Simplified design of steerable pyramid filters," in *Proc. IEEE ISCAS*, 1998.
- [7] R. D. Nowak and R. G. Baraniuk, "Wavelet-domain filtering for photon imaging systems," *IEEE Trans. Image Processing*, pp. 666 –678, May 1999.
- [8] J.-L. Starck, F. Murtagh, and A. Bijaoui, *Image Processing and Data Analysis, the multiscale approach*, Cambridge University Press, 1998, 2000.
- [9] L. Şendur and I. W. Selesnick, "Bivariate shrinkage functions for wavelet-based denoising exploiting inter-scale dependency," *IEEE Trans. Signal Processing*, vol. 50, no. 11, pp. 2744 –2756, November 2002.
- [10] S. Mallat, *A wavelet tour of signal processing (2nd ed.)*, Academic Press, Oval Road, London, 1998,1999.
- [11] R. Molina, J. Núñez, F. J. Cortijo, and J. Mateos, "Image restoration in astronomy, a bayesian perspective," *IEEE Signal Processing Magazine*, pp. 11–29, March 2001.